Thermal conductivity and temperature in solid argon by nonequilibrium molecular dynamics simulations

P. Heino
Tampere University of Technology, Institute of Electronics, P.O. Box 692, FIN-33101 Tampere, Finland
(Received 30 November 2004; revised manuscript received 4 February 2005; published 28 April 2005)

The phonon density of states in equilibrium and nonequilibrium solid argon was analyzed with the molecular-dynamics method and using the Lennard-Jones interaction. The computational method was validated by comparing the thermal conductivity and its finite-size effect to reference data. A small, but statistically significant, difference between the phonon density of states in thermal equilibrium and in a nonequilibrium stationary state was observed. The phonon density of states was used to characterize the local lattice temperature in the nonequilibrium case. The results were compared to the local temperature, as defined by the average kinetic energy.

DOI: 10.1103/PhysRevB.71.144302 PACS number(s): 63.22.+m, 31.15.Qg, 65.80.+n

I. INTRODUCTION

Recent advances in synthesis, processing, and microanalysis are enabling the routine production of well characterized materials with a structure that varies on the length scale of several nanometers. In this length scale, the size is comparable with the mean free path of phonons, and the thermal properties become affected by the system size. Therefore, microscale and nanoscale thermal conduction has received a lot of interest in the past two decades.[1–4]

In macroscale, thermal conduction is treated as a material property, and energy transfer is calculated simply with the *phenomenological* Fourier law derived in the early 1800s.[5] The validity of the Fourier law breaks down if (i) the size scale is less than the mean free path of energy carriers, (ii) the time scale is shorter than the relaxation time, or (iii) temperature is close to zero.[5] In many practical applications, such as superlattices, polymer nanocomposites, multilayer coatings, microelectromechanical systems, and micro- and optoelectronic devices, only the size scale limits the Fourier law.

In small length scales, thermal conduction can be calculated with the Boltzmann transport equation (BTE).[3] The solution of BTE falls into three classes: directly solving the BTE as a partial differential equation,[6] using Monte Carlo methods to obtain the solution,[7] or using results from (photon) radiative heat transfer.[8] In the BTE approach, the physics of heat transfer and phonon scattering are incorporated explicitly in the calculations. Thus, for a reliable calculation, a good understanding of the fundamental phonon processes and relaxation times is required. In some cases (e.g., point defects), these are well known, but in others (e.g., interfaces) this is not the case.[2]

In addition to BTE, the molecular-dynamics method (MD) is emerging as a tool for studying thermal conduction at the microscale.[2,9] With MD the thermal conductivity can be calculated from equilibrium calculations, from a known heat flux and temperature gradient,[9] or from temperature decay calculations.[10] It is best suited for studying the effect of structural imperfections (boundaries, dislocations, grain boundaries, voids, interstitials, etc.) on the thermal conductivity. In addition to conductivity calculations, MD can be used to calculate the temperature-dependent phonon spectral distribution.[11] In the molecular-dynamics method, the trajectories of atoms or molecules in the system are numerically solved. Generally, the main problem with MD is to find the accurate interaction between atoms in the system of interest. In classical MD, the forces acting on atoms are derived from a classical interaction potential, while in *ab initio* methods the forces are derived from first principles, i.e., from electron states and bonding. Sometimes structural energy calculations are performed with *ab initio* calculations, and a parametrized classical potential is then fitted to these data to obtain a reasonably accurate and computationally feasible potential.[12,13]

In microscopic nonequilibrium calculations, the definition of temperature is not well established. Classically, in equilibrium, it can be defined from the average kinetic energy of particles.[14] This is not a problem, since, in equilibrium, averaging over time or population should yield the same result. However, in the presence of a temperature gradient, what is the volume over which the averaging should be done? In MD calculations, the spatial accuracy is often taken to extremes, and a local temperature can be defined for each atom from its time-averaged kinetic energy. However, the concept of phonons introduces two length scales: the wavelength and the mean free path (MFP). As collisions within the distance of the MFP are needed for the equilibrium population of heat carriers to exist, two regions with different temperatures must be at least a distance of MFP away from each other.[2]

At the microscale, temperature gradients are commonly generated by hot spots, e.g., in transistors.[6] In these cases, the system is not in equilibrium, since diffusive heat transfer requires the length scale to be much greater than the MFP. If the length scale is smaller, the number of scattering events in the hot spot is reduced by the size of the spot. Then, outside the hot spot the heat carriers leaving the spot are *not in thermal equilibrium* with the carriers entering the spot. This effect has been studied by Chen in Ref. 15, where the BTE was solved with radiation equations. When the size of the hot spot is small, temperature has a discontinuity at the boundary of the hot spot. This is due to the nonequilibrium nature of heat transfer. In the limit of no scattering, i.e., ballistic trans-

port between a cold and a hot spot, heat carriers from two different temperatures *should exist simultaneously*.[8,15] Scattering drives these two temperatures towards an equilibrium temperature, but happens only on the length scale of the MFP. The aim of this paper is to characterize the local temperature in nonequilibrium molecular-dynamics simulations including hot spots.

II. EQUILIBRIUM SIMULATIONS

A. The model

Molecular dynamics is used to describe the lattice vibrations in the system. As the main interest is in vibrational properties of the system, general size effects, and thermal conduction by phonons, the system is described using the classic Lennard-Jones (6-12) potential,

$$\phi_0(r) = 4\epsilon\left[\left(\frac{\sigma}{r}\right)^{12} - \left(\frac{\sigma}{r}\right)^{6}\right]. \quad (1)$$

In this work, periodic boundaries and parameters for solid argon are used. For computational reasons, the potential is cut at a reasonably large distance, which slightly modifies the potential. The interaction potential used in the calculations is given in detail in Appendix A.

B. Phonon density of states (DOS)

Phonons are quanta of lattice vibrations. In MD simulations, phonons are not explicitly simulated. The motion and vibration of atoms are simulated, and phonon statistics can be gathered from the analysis of lattice vibrations. These vibrations are commonly characterized by the phonon density of states (DOS), which describes the amount of vibrations at different frequencies. It is calculated from the velocity-velocity autocorrelation function by Fourier transform.[17] Specifically, the DOS is calculated from[18,19]

$$\omega G = \frac{M}{\pi k_B T}\int_0^\infty dt\, \cos(\omega t) e^{-(t/\tau)^2}\langle \vec{v}(t)\vec{v}(0)\rangle. \quad (2)$$

Here the exponential window is explicitly written out, G is the DOS, ω the frequency, M the mass, k_B the Boltzmann constant, T the temperature, and $\langle\ldots\rangle$ the velocity-velocity autocorrelation function. The cosine integral was obtained from the real part of the fast-Fourier-transform (FFT) coefficients. The autocorrelation function was obtained with MATLAB software, which uses the Wiener-Khinchin theorem[20] (i.e., FFT) to speed up the computations. The DOS in equilibrium temperatures 5, 10, 15, 20, …, 75, and 80 K were calculated using the window $\tau = 20$ ps. These functions are shown in Fig. 1. In these equilibrium calculations, the autocorrelation was calculated from 1 million time steps (time step $\Delta t = 6.6$ fs) as an average over 50 atoms in a 2200-atom system. The DOS of solid argon in 25 K has been calculated also, e.g., in Ref. 17, and the results are similar. This shows that the DOS is not heavily dependent on the system size, since most likely the systems sizes were different in Ref. 17.

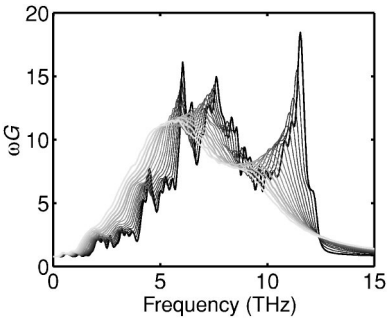

FIG. 1. Phonon density of states as a function of frequency and temperature given in nine temperatures: $T = 5$ K (black), 10 K, 15 K, …, 75 K, and 80 K (light gray).

From Fig. 1, the effect of temperature on the DOS is clearly seen. The system in a low temperature seems to have some well defined peaks in the DOS, while in higher temperatures these peaks are not present. This can be related to the disordered structure: the higher the temperature, the more fluctuations from the fcc structure. There is also a tendency towards lower frequencies with increasing temperature. This is most likely due to thermal expansion and anharmonic effects. The spring constant of each bond, i.e., the second derivative of the bond energy, depends on the bond length, as depicted in Fig. 2. For the nearest neighbors in $T = 5$ K, the spring constant is approximately $k = 12$ GN/m. As there are 12 nearest neighbors in the fcc structure, a frequency of the order of $\sqrt{12k/m}$, where m is the mass of the atom, is expected. For solid argon this gives $\omega = 15$ THz. As the bonds lie in six different directions, their addition is indeed questionable, and thus this frequency is greater than the frequency of the peak in Fig. 1, even if relatively close. At the temperature $T = 80$ K, the thermal expansion increases the bond length, and decreases the spring constant to approximately 5 GN/m, as depicted in Fig. 2. This decreases the order of magnitude estimate of the frequency to $\omega = 9.5$ THz. Both these frequency estimates are quite close to the high frequencies shown in Fig. 1. Thus, it seems that the frequency reduction is due to thermal expansion and anharmonic properties of the potential. In a high temperature, the peaks become distorted due to structural fluctuations, which widen the bong length and spring constant distributions.

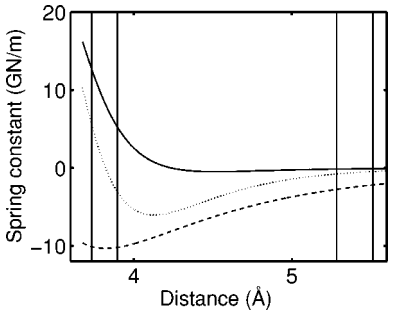

FIG. 2. Energy (dashed line, arb. units), force (dotted line, arb. units), and spring constant of a bond as a function of interatomic distance. The nearest-neighbor and next-nearest-neighbor distances for $T = 5$ K and $T = 80$ K are shown with vertical lines.

The functions presented in Fig. 1 are not simply linear combinations of each other. Thus, e.g., a system consisting of both 60 K and 20 K particles has a different DOS than a system consisting of only 40 K particles. This enables the calculation of several temperatures (i.e., a distribution of temperatures) from a single DOS. Moreover, since the DOS can be calculated from a single location (atom), in principle, a local temperature distribution can be assigned to each location. As motivated in the Introduction, in a nonequilibrium system, the heat carriers, i.e., phonons, are excited in different temperatures. In the microscale, these phonons are not scattered towards an equilibrium temperature, because there is not enough space for scattering. Thus, in a single location, phonons from several temperatures could exist simultaneously, and their temperature should be described with a local temperature distribution.

III. NONEQUILIBRIUM SIMULATIONS

In nonequilibrium simulations, a constant heat flux was used, as proposed by Jund and Jullien.[21] The size of the system in one direction was varied between 12 nm and 3900 nm, while in the other two directions the system size was five lattice constants. In another study, the thermal conductivity has been seen to be independent of the system size in the other two directions, within the error inherent in the calculations.[9] This shows that the phonon statistics in the system is not heavily dependent on these system sizes. Periodic boundaries were used in all directions, and the number of atoms in the systems was between 2000 and 64 000. The constant heat flux was selected so that the temperature interval was roughly 20–60 K. In practice, the flux depended on system size, and was between 0.19 and 1.5 GW m^{-2}.

A. Thermal conductivity

In nonequilibrium MD simulations, the thermal conductivity of the system can be calculated directly from the Fourier law,

$$j = -\kappa \nabla T, \tag{3}$$

where j is the heat flux, ∇T the temperature gradient, and κ the thermal conductivity. In this section, the local temperature is calculated from the atoms' kinetic energy as an average over time and in a narrow region. As an example, the temperature profile and the region in which the averaging is done are shown in Fig. 3.

As seen from the inset in Fig. 3, the temperature gradient is not constant. This is due to the temperature dependence of thermal conductivity of solid argon, which is nearly linear.[16] Thus a second degree polynomial was fitted to the temperature profile, for 25 K $< T <$ 55 K, to obtain the conductivity. In what follows, thermal conductivity is evaluated in the mean temperature, i.e., $T = 40$ K.

The thermal conductivity, as calculated from Eq. (3), was seen to be practically independent of the heat flux. However, the results were heavily dependent on the system size. The size dependence is due to the phonon scattering locations induced in the system by the heating and cooling regions. By decreasing the MFP, these regions should scale the thermal conductivity as[9,22]

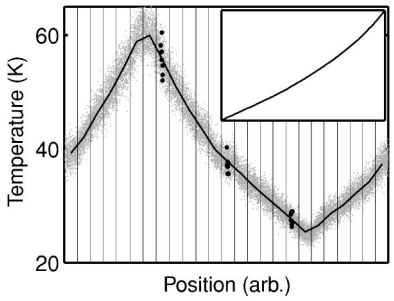

FIG. 3. Temperature profile in a Lennard-Jones system. The gray dots indicate particles' local temperature as a time average over 154 ps, the vertical lines are the limits for spatial averaging, and the solid black line is the local temperature calculated as the spatio-temporal average of the atoms. The inset shows a 6 ns spatio-temporal average, where the two profiles are also averaged. The black dots indicate atoms which are used to calculate the nonequilibrium phonon density of states (cf. text).

$$\frac{1}{\kappa} = \frac{2}{nk_B v}\left(\frac{1}{l_\infty} + \frac{4}{L}\right). \tag{4}$$

Here κ is the thermal conductivity, n is the number density of atoms, k_B the Boltzmann constant, v the average group velocity of acoustic phonon modes, l_∞ the phonon mean free path in an infinite system, and L the system size. The number density, n, in an fcc system is $4/d^3$, where d is the lattice constant. The data obtained from simulation are shown in Fig. 4. By fitting Eq. (4) to these data, the size dependence can be found, and by extrapolating down to $1/L = 0$ the bulk thermal conductivity can be obtained. In this case, the conductivity is 0.55 W/mK. In Ref. 16, a thermal conductivity of approximately 0.54 W/mK was obtained for Lennard-Jones solid argon by Green-Kubo simulations. The results are nearly identical. In another work, where the finite-size effects of solid argon were studied, the conductivity 0.604 W/mK was obtained.[22] This is also in good agreement with the present results. The difference between the simulated conductivities may be related to the different cutoff distances used for the potential. The experimental value is about 0.74 W/mK.[23] The difference between the simulated

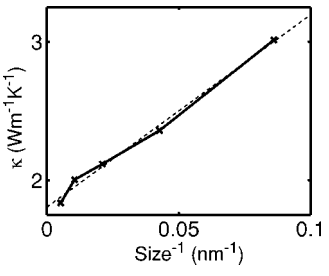

FIG. 4. Thermal conductivity of solid argon at 40 K, as a function of system size. The dashed line is a best fit to the data [cf. Eq. (4)]. Bulk thermal conductivity can be extrapolated from $1/L = 0$, and is in agreement with other simulations and experimental data (Refs. 16 and 23).

and experimental conductivity is relatively large. One possible explanation is that classical MD simulations for conductivity should be valid only in high temperatures. In this case, the temperature is less than half of the Debye temperature, and thus some phonon modes are excited in the MD simulations that are not excited in the real solid.

In addition to thermal conductivity, the average speed of acoustic phonons and the mean free path of phonons can be found from the coefficients in Eq. (4). Estimates for argon in $T=40$ K are $v=1500$ m/s and $l_\infty=2$ nm. The average speed of acoustic phonons is related to the Debye temperature, θ_D, as[16]

$$v = \frac{k_B \theta_D}{\hbar k_D}, \tag{5}$$

where k_B is the Boltzmann constant, $\hbar$ the Planck constant, and $k_D=\sqrt[3]{6N\pi^2/V}$ the Debye wave vector. Inserting the Debye temperature $\theta_D=92$ K,[24] 1000 m/s is obtained for the speed of acoustic phonons. In addition, in Ref. 25 experimental values of around 1000 m/s were cited. Moreover, based on data in Refs. 16 and 23, the phonon mean free path in $T=40$ K can be estimated to be around 2 nm. In Ref. 22, a MFP of 3.4 nm was obtained in 40 K. Therefore, the values obtained from the finite-size effects of thermal conductivity, i.e., $v=1500$ m/s and $l_\infty=2$ nm, are also in agreement with reference values.

B. Temperature characterization

In the previous section, the local temperature was calculated directly from the average kinetic energy. As motivated above, in microscopic systems with hot spots, the lattice (i.e., the phonons) should be in several different temperatures simultaneously. This is due to the small length scale: phonons do not have enough space to scatter to equilibrium. Thus phonons from hot regions should be present in a cold region and vice versa. As discussed above, the phonon densities of states in equilibrium systems with different temperatures are *not* linearly dependent. This opens up the possibility to calculate a local temperature distribution from the DOS. As the DOS can be calculated entirely locally, in principle, a local temperature distribution can be calculated.

A most important question is, is the equilibrium DOS different from nonequilibrium DOS? Moreover, as the velocity-velocity autocorrelation function is calculated as an average, is the difference statistically meaningful? In Fig. 5, the velocity-velocity autocorrelation function is shown both for the nonequilibrium case, with the *local* temperature 40 K, and the equilibrium case, with the temperature 40 K. In the figure, these functions completely overlap. There is a small difference, as shown in Fig. 5, where the difference is multiplied by a factor of 100. As seen in the figure, the difference between autocorrelation functions in equilibrium and nonequilibrium systems is around 1%. Long simulation times were used in these simulations. For example, for the data of the figure, a nonequilibrium system was tracked for more than 3 million time steps, and the autocorrelation was calculated from 3 million time steps. Because of the long simulation time, and since the autocorrelation is an average over

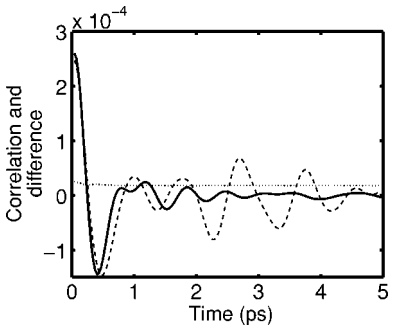

FIG. 5. Velocity-velocity autocorrelation function for short time differences (solid line) in $T=40$ K. The difference between nonequilibrium and equilibrium cases is invisible. Dashed line shows the difference, magnified by a factor of 100. Although small, this difference is still much larger than statistical error (300 times standard deviation is shown by dotted line).

time, the standard deviation becomes minute. In the figure, the standard deviation is multiplied by 300, so the difference can easily be seen to be much greater than three times the standard deviation. Most often the difference is about 5–15 times the standard deviation. Thus, it is seen that with these simulation times and number of atoms recorded, the difference is statistically meaningful, even if small. In Ref. 17, Chantrenne and Barrat concluded that the difference between velocity distributions in equilibrium and nonequilibrium simulations is not significant, since the difference was less than 2%. However, they used much shorter simulation times and smaller temperature gradients. In this case the difference is around 1%, but still meaningful.

To test the possibility of calculating a local temperature distribution from the DOS, three regions in the nonequilibrium simulations were chosen to represent hot, cold, and medium temperature atoms. A total of 25 atoms were selected, as depicted in Fig. 3. The autocorrelation over 1.5–3 million time steps and eight or nine atoms was calculated to obtain the DOS. (In all cases, over 3 million time steps were tracked. However, in large systems, a longer initial period was needed to obtain a stationary temperature profile.) A linear combination of equilibrium DOS was optimized to fit the calculated nonequilibrium DOS. The coefficients of the equilibrium DOS represent the local temperature distribution. Details of the optimization procedure are presented in Appendix B.

As an example, DOS from the second smallest system of Fig. 4 ($L=23$ nm) are shown in Fig. 6. In the figure, the light curve corresponds to an average of eight hot atoms (local temperature as calculated from the spatio-temporal averaged kinetic energy is $T_{\mathrm{MD}}=49.5$ K). The other curves are for nine atoms with $T_{\mathrm{MD}}=39.8$ K and eight atoms with $T_{\mathrm{MD}}=32.0$ K. The black line is the average of these three with $T_{\mathrm{MD}}=40.4$ K. In Table I, the local temperature distributions, as obtained by optimization and corresponding to these DOS, are presented. The average local temperatures calculated from these distributions are 46.4, 39.6, 34.6, and 40.2 K. As compared to the local temperature values calculated from the kinetic energy, these values are extremely good.

It is emphasized that, even if the local temperature calculated from the kinetic energy is extremely close to a calcu-

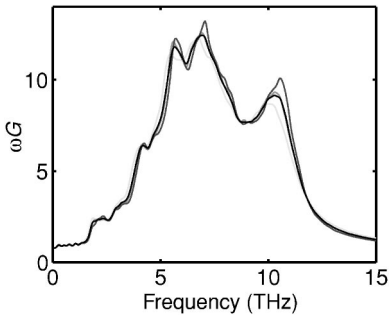

FIG. 6. Phonon density of states as a function of frequency in a small system. The DOS correspond to hot (light) or cold (dark) atoms. An average is also shown (black).

lated equilibrium temperature, e.g., the middle atoms—$T_{\mathrm{MD}}=39.8\ \mathrm{K}\approx 40\ \mathrm{K}$—the DOS does not equal the DOS of the same equilibrium temperature. The DOS of the nonequilibrium case suggest a slightly wider local temperature distribution. The difference of autocorrelation functions in this case was discussed above, and shown in Fig. 5. Moreover, the temperature, T_{MD}, as calculated from the kinetic energy of *all* 25 atoms (i.e., an average of three local temperatures), is 40.4 K, and very close to the temperature in the central region. However, the temperature distribution as calculated from the DOS is much wider, since the DOS includes contributions from all three locations.

Interestingly, the hot region seems to contain some ($\approx 5\%$) phonons from the cold region, and the cold region seems to contain some ($\approx 3\%$) phonons from the hot region. This is qualitatively in agreement with the phonon relaxation model: some phonons leaving the cold region can travel ballistically (i.e., without scattering) to the hot region (and vice versa), because the dimension of the system is not very much larger than the mean free path of phonons. Similar behavior was seen also in other systems. However, increasing the system size from 23 nm to 380 nm does not significantly change the percentage of the cold phonons, as the scattering model suggests. As an example, in Table II the analysis is repeated for a four-times-larger system. Again there are some cold atoms present in the hot region. However, the fraction is

TABLE I. Optimization results in the case of Fig. 6. $L=23$ nm.

	Hot (%)	Middle (%)	Cold (%)	Average (%)
$T=20$	5.0	0	0	1.2
$T=25$	0	0	0	0
$T=30$	0	0	16.5	6.8
$T=35$	0	10.7	80.8	25.1
$T=40$	0	85.8	0	37.2
$T=45$	57.6	3.5	0	16.0
$T=50$	24.6	0	2.7	11.4
$T=55$	13.9	0	0	0
$T=60$	0	0	0	2.2
T_{MD}	49.5	39.8	32.0	40.4
T_{mean}	46.4	39.6	34.6	40.2

TABLE II. Optimization results in an $L=100$ nm system.

	Hot (%)	Middle (%)	Cold (%)	Average (%)
$T=20$	7.4	0	0	0
$T=25$	0	0	0	3.3
$T=30$	0	0	80.3	26.7
$T=35$	0	29.9	19.6	16.4
$T=40$	3.2	67.3	0	19.0
$T=45$	0	2.8	0	0
$T=50$	35.2	0	0	28.3
$T=55$	44.9	0	0	0
$T=60$	12.4	0	0	6.4
T_{MD}	55.8	37.9	27.3	40.3
T_{mean}	51.2	38.6	30.9	40.1

about the same order as previously. In the average distribution, the peaks near the T_{MD} temperatures 55, 38, and 28 K are shifted to 50, 40, 35, and 30 K, but can be observed.

IV. DISCUSSION

These results show that the DOS in equilibrium and nonequilibrium MD simulations are different, even if the difference is only around 1%. From 3 million time steps and nine atoms in a nonequilibrium system, the difference was typically 5–15 times the standard deviation, and therefore statistically meaningful results were obtained. Based on these calculations, the results from 3 million times steps should be meaningful also for a single atom. In these nonequilibrium systems, the number of atoms in the same environment (i.e., temperature) is limited by the small system size in the directions perpendicular to the heat flux. Therefore, long simulation times are necessarily needed even if large systems are used. In another study, Chantrenne and Barrat studied nonequilibrium solid argon, and concluded that the velocity distribution of nonequilibrium systems did not differ significantly from the equilibrium (Maxwell) distribution.[17] However, in their simulations a much smaller temperature difference was imposed in the system, and significantly shorter periods of time were simulated.

The results suggest that a local temperature distribution can be calculated for each location from the DOS in nonequilibrium MD, and that the average of this distribution is very close to the local temperature calculated from the kinetic energy. The results can be useful in calculating relaxation times from MD simulations. The relaxation times are needed, e.g., in the solution of BTE.

One may ask, is it reasonable to use the equilibrium DOS as a basis when dealing with a nonequilibrium system? It might prove informative to study the DOS in different locations and study, e.g., the relaxation times directly from the DOS, and not try to fit any equilibrium DOS to the nonequilibrium DOS. However, this paper was intended to clarify some of the problems characterizing the temperature in nonequilibrium microscale systems.[2]

V. SUMMARY

The phonon density of states was calculated in solid argon in different equilibrium temperatures and in different non-

equilibrium cases. In a nonequilibrium system, for a given *local* temperature, the phonon density of states (DOS) was *not* equal to the DOS of an equilibrium system in the same temperature. Moreover, the equilibrium DOS were linearly independent of each other. An optimization procedure was outlined to calculate a temperature distribution from the DOS. This procedure was used to calculate local temperature distributions from the nonequilibrium DOS. The averages of these distributions were extremely close to the local temperatures calculated from the kinetic energy, even though the nonequilibrium DOS could not be represented by a single temperature peak in the distribution. It was shown that in nonequilibrium molecular-dynamics simulations, the local temperature can be obtained in two ways: from the average kinetic energy or from the DOS. Both of these approaches are entirely local, but the latter reflects the nonequilibrium nature of phonons in microscale systems. These temperature distributions might prove useful in calculating the phonon scattering rates from MD simulations.

ACKNOWLEDGMENT

This work has been funded by the Academy of Finland.

APPENDIX A: DETAILS OF THE POTENTIAL

The interaction between noble gas atoms can be described using the classical Lennard-Jones potential,

$$\phi_0(r) = 4\epsilon\left[\left(\frac{\sigma}{r}\right)^{12} - \left(\frac{\sigma}{r}\right)^{6}\right]. \tag{A1}$$

In this work, parameters for solid argon are used: $\sigma = 3.405$ Å and $\epsilon/k_B = 119.8$ K.[16] For computational reasons, the potential is cut at the cutoff, r_c, which is chosen "large enough," so that the interaction at this distance is negligible. In principle, the potential can be cut by adding the cutting point energy (which creates a discontinuity for the force, e.g., Ref. 26), by introducing a distance-dependent correction term and zero-point energy for the whole range,[27] or to use a different potential at the cutoff range, e.g., by multiplying the potential[28] or by correcting its parameters.[29] What one typically wants from the cutoff procedure is that the forces and energy go to zero at the cutoff distance, and that forces and energy are continuous. Moreover, the original potential should be modified as little as possible. Motivated by the traditional polynomial correction[27] and the smooth cutting procedures,[28,29] the Lennard-Jones potential is corrected at a certain range by a polynomial. Thus, the following potential is used:

$$\phi(r) = \begin{cases} \phi_0(r), & r < r_s \\ \phi_0(r) - P(r), & r_s \leqslant r \leqslant r_c \\ 0, & r > r_c. \end{cases} \tag{A2}$$

Here $P(r)$ is a corrective polynomial which is defined by the needs discussed above,

$$P(r_s) = 0, \tag{A3}$$

$$P'(r_s) = 0, \tag{A4}$$

$$P(r_c) = \phi_0(r_c), \tag{A5}$$

$$P'(r_c) = \phi_0'(r_c). \tag{A6}$$

Here r_s is the lower limit, where the cutoff starts, and r_c is the cutoff distance. A third-degree polynomial satisfies the constraints, and its coefficients can easily be calculated from the constraints, e.g., with symbolic mathematics software such as MAPLE. In this work, the standard cutoff, $r_c = 2.5\sigma$, was selected.[30] The distance to start cutoff is chosen so that the force in the whole cutoff range is decreasing, specifically in this work $r_s = 2.0\sigma$. The effect of a narrower cutoff would be that the force increases at the range $r_s < r < r_c$. This effect could be minimized also by subtracting $\phi_0(r_c)$ from the energy *for all r*, and requiring $P(r_c) = 0$.

APPENDIX B: OPTIMIZATION

Consider a system which consists of atoms in equilibrium temperatures T_i. Let the fractions in each temperature, p_{T_i}, be tabulated in a column vector $\vec{T} = [p_{T_1} p_{T_2} \cdots p_{T_N}]$. Let $\vec{\mathrm{DOS}}_{T_i}$ be the DOS of atoms at the equilibrium temperature T_i. Here the DOS (function) is represented by its discretized column vector. Now, since autocorrelation and FFT are linear operations, the DOS of this system can be calculated simply by the weighed sum,

$$\vec{\mathrm{DOS}} = \sum_i p_{T_i} \vec{\mathrm{DOS}}_{T_i} = [\vec{\mathrm{DOS}}_{T_1} \vec{\mathrm{DOS}}_{T_2} \cdots \vec{\mathrm{DOS}}_{T_N}]\vec{T}. \tag{B1}$$

From the nonequilibrium MD simulations, a DOS is obtained. Let it be denoted by $\vec{\mathrm{DOS}}_{\mathrm{MD}}$. If this distribution is to be represented by a system of atoms in different equilibrium temperatures, this DOS should be represented by some linear combination of the equilibrium DOS, as discussed above. Thus, the temperature distribution can be found by minimizing the error,

$$\vec{e} = \vec{\mathrm{DOS}}_{\mathrm{MD}} - [\vec{\mathrm{DOS}}_{T_1} \vec{\mathrm{DOS}}_{T_2} \cdots \vec{\mathrm{DOS}}_{T_N}]\vec{T}. \tag{B2}$$

Here $\vec{\mathrm{DOS}}_{\mathrm{MD}}$ is the calculated nonequilibrium DOS, expressed in a column vector, $\vec{\mathrm{DOS}}_{T_i}$ is the calculated DOS in the equilibrium temperature T_i, $\vec{e}$ is the error, and $\vec{T}$ is the temperature distribution (vector). Since the equilibrium DOS are linearly independent, the simulated DOS can be represented by a unique linear combination of equilibrium DOS. The value of $\vec{T}$ is obtained by minimizing the norm of $\vec{e}$. In this equation, the vectors $\vec{\mathrm{DOS}}_{T_i}$ (discretized functions) form the basis, and the functions ωG were used, since the division by ω would have significantly weighed the low-frequency DOS. DOS in the temperatures $T = 20$ K, 25 K, 30 K, …, 60 K were included in the basis.

As seen from Fig. 1, the difference of different $\vec{\mathrm{DOS}}_{T_i}$ is

not large, and thus numerical problems may rise. To improve accuracy, another basis was chosen for the optimization. As the first basis function, the mean DOS was chosen. The second basis function was the DOS of the coldest atoms minus its projection to the known (new) basis. In the first step, only the average DOS is in the basis. The third basis function was the DOS of the second coldest atoms minus its projection to the known (new) basis, etc. The optimization was done by minimizing the sum of absolute error, i.e., the 1-norm, by using the MATLAB software. In addition, the following restrictions were imposed. First, the factors of $\vec{\mathrm{DOS}}_{T_i}$ should be non-negative (i.e., at least zero phonons must correspond to a specified temperature). Second, the factors must sum up to 1. Both these restrictions apply in the original DOS basis, not the one used in optimization. These restrictions were implemented in the error function as additional terms, and thus were not satisfied exactly. Moreover, in the course of optimization, the basis was reduced iteratively. After each optimization round, the $\vec{\mathrm{DOS}}_{T_i}$ that corresponded to the temperature, where the population was lowest and below 1%, was removed from the basis. This was repeated until each calculated population exceeded 1%.

[1] K. E. Goodson and Y. S. Ju, Annu. Rev. Mater. Sci. **29**, 261 (1999).

[2] D. G. Cahill *et al.*, J. Appl. Phys. **93**, 793 (2003).

[3] C.-L. Tien, A. Majumdar, and F. M. Gerner, *Microscale Energy Transport* (Taylor & Francis, Washington, D.C., 1998).

[4] G. Chen, D. Borca-Tasciuc, and R. G. Yang, *Nanoscale Heat Transfer in Encyclopedia of Nanoscience and Nanotechnology* (American Scientific Publishers, Valencia, CA, 2004), http://web.mit.edu/ronggui/www/publications.html.

[5] K. K. Tamma and X. Zhou, J. Therm. Stresses **21**, 405 (1998).

[6] P. D. Sverdrup, Y. Sungtaek-Ju, and K. E. Goodson, J. Heat Transfer **123**, 130 (2001).

[7] S. Mazumder and A. Majumdar, J. Heat Transfer **123**, 749 (2001).

[8] G. Chen, Phys. Rev. B **57**, 14 958 (1998).

[9] P. K. Schelling, S. R. Phillpot, and P. Keblinski, Phys. Rev. B **65**, 144306 (2002).

[10] B. C. Daly, H. J. Maris, K. Imamura, and S. Tamura, Phys. Rev. B **66**, 024301 (2002).

[11] C. Z. Wang, C. T. Chan, and K. M. Ho, Phys. Rev. B **42**, 11 276 (1990).

[12] M. Z. Bazant, E. Kaxiras, and J. F. Justo, Phys. Rev. B **56**, 8542 (1997).

[13] Y. X. Shen, H. R. Gong, L. T. Kong, and B. X. Liu, J. Alloys Compd. **366**, 205 (2004).

[14] M. Alonso and E. J. Finn, *Fundamental University Physics* (Addison-Wesley, Reading, MA, 1968).

[15] G. Chen, J. Heat Transfer **118**, 539 (1996).

[16] K. V. Tretiakov and S. Scandolo, J. Chem. Phys. **120**, 3765 (2004).

[17] P. Chantrenne and J.-L. Barrat, J. Heat Transfer **126**, 577 (2004).

[18] P. Gumbsch and M. W. Finnis, Philos. Mag. Lett. **73**, 137 (1996).

[19] C.-K. Loong *et al.*, Phys. Rev. B **45**, 8052 (1992).

[20] *Mathworld*, edited by E. W. Weisstein (Wolfram Research, http://mathworld.wolfram.com/, 2004).

[21] P. Jund and R. Jullien, Phys. Rev. B **59**, 13 707 (1999).

[22] S.-H. Choi, S. Maruyama, K.-K. Kim, and J.-H. Lee, J. Korean Phys. Soc. **43**, 747 (2003).

[23] D. K. Christen and G. L. Pollack, Phys. Rev. B **12**, 3380 (1975).

[24] C. Kittel, *Introduction to Solid State Physics*, 5th ed. (Wiley, NY, 1976).

[25] S. Volz, J.-B. Saulnier, M. Lallemand, B. Perrin, P. Depondt, and M. Mareschal, Phys. Rev. B **54**, 340 (1996).

[26] M. J. D. Brakkee and S. W. deLeeuw, J. Phys.: Condens. Matter **2**, 4991 (1990).

[27] F. Shimizu, H. Kimizuka, H. Kaburaki, J. Li, and S. Yip, Parallel Molecular Dynamics Simulation on Elastic Properties of Solid Argon, in Proceedings of the 4th International Conference on Supercomputing in Nuclear Applications, Tokyo, Japan, 2000.

[28] J. Mei, J. W. Davenport, and G. W. Fernando, Phys. Rev. B **43**, 4653 (1991).

[29] J. Q. Broughton and G. H. Gilmer, J. Chem. Phys. **79**, 5095 (1983).

[30] D. C. Rapaport, *The Art of Molecular Dynamics Simulation*, 2nd ed. (Cambridge University Press, Cambridge, 2004).